UDC 539.3

A. P. Yankovskii ✉

MODELING OF THERMOELASTOPLASTIC DEFORMATION OF REINFORCED PLATES. II. STATEMENT OF THE PROBLEM AND METHOD FOR SOLUTION

A coupled initial-boundary value problem of thermoelastoplastic deformation of flexible reinforced plates is formulated. The possible weak resistance of such structures to transverse shear is taken into account within the framework of the Ambartsumian theory. Geometric nonlinearity is taken into account in the von Kármán approximation. The temperature over the thickness of the plates is approximated by polynomials of different orders. The solution to the two-dimensional problem is constructed using an explicit numerical scheme. The dynamic thermoelastoplastic behavior of plane criss-cross and spatially reinforced fiberglass and metal-composite plates, bending under the action of an air blast wave, is investigated. It is shown that in order to adequately determine the temperature in such structures, it must be approximated by polynomials of the 6–7th orders over the thickness of the plates. It is demonstrated that relatively thin composite plates are heated to a larger extent than relatively thick ones at the same maximum values of the intensity of deformations in the binder. The heating level of reinforced structures is insignificant: for fiberglass plates, the temperature increment is 2÷18°C*, and for metal-composite structures, it is* 30°C*. Therefore, the dynamic calculation of fiberglass plates under the action of a load such as an air blast wave can be carried out without taking into account the thermal effect in the absence of additional heat sources of non-mechanical origin. In calculating the metal-composite plates, it is necessary to take into account the thermal effect, but the thermal sensitivity can be ignored.*

Key words: *flexible plates, plane reinforcement, spatial reinforcement, dynamic bending, Ambartsumian's theory, thermoelastoplastic deformation, explosive-type load, explicit numerical scheme.*

This paper continues the study published in [24], where a numerical-analytical structural model of thermoelastoplastic deformation of a fiber-reinforced material is developed using the constitutive equations of the theory of plastic flow for the components of the composition. In this case, the loading surfaces of the materials of the composition are assumed to be depend not only on the parameters of reinforcement, but also on the temperature. The structural model of a composite material (CM) proposed in [24] is focused on the use of explicit numerical schemes for solving coupled problems of thermoelastoplasticity.

The present study is devoted to the formulation of the coupled problem of thermoelastoplastic bending deformation of CM-plates, taking into account their possible weak resistance to transverse shears, to the development of explicit numerical methods for integrating the corresponding initial boundary-value problems, and to a discussion of the calculation results. A review of the relevant publications is given in [24].

1. Simulation of thermoelastoplastic deformation of a flexible reinforced plate. Let us consider the bending behavior of a CM-plate with a thickness $2h$ (Fig. 1), refereed to a Cartesian rectangular coordinate system $Ox_1x_2x_3$: Ox_1x_2 is a middle plane; the axis Ox_3 is transverse ($|x_3| \le h$). The structure can be reinforced plane criss-cross (Fig. 1***a***) or spatially (Fig. 1***b***) with N families of fibers in arbitrary directions with densities of reinforcement ω_k, $1 \le k \le N$. In the direction Ox_3, the structure of the reinforcement is quasihomogeneous.

✉lab4nemir@rambler.ru

To simulate a possible weak resistance of a flexible CM plate to transverse shear (for example, in cases of plane criss-cross reinforcement structures or in the case of a spatial reinforcement structure shown in Fig. 1***b***, under shear in a plane Ox_1x_3), we use Ambartsumian's theory [2, 20, 23], and the geometric nonlinearity of the problem we take into account in the von Kármán approximation.

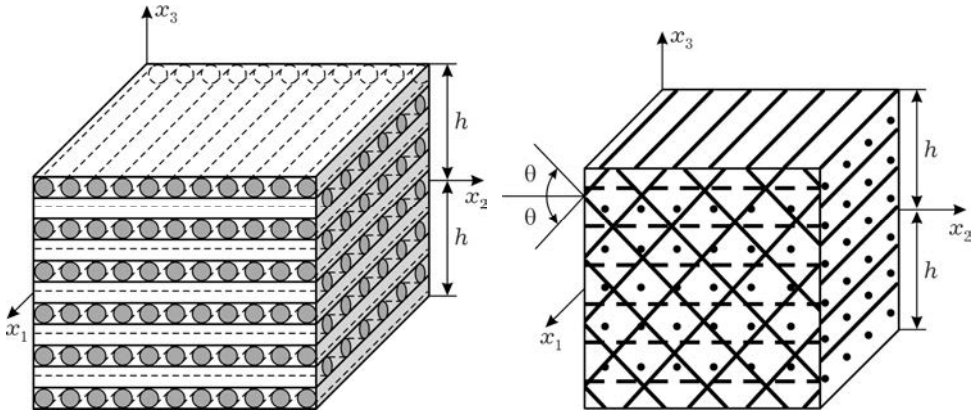

a) ***b***)

Fig. 1. Element of a CM-plate: ***a***) – plane orthogonal reinforcement; ***b***) – spatial reinforcement in four directions.

Remark. It was shown in [21] that in the case of elastoplastic deformation of thin-walled structural elements with arbitrary spatial reinforcement structures, it is not possible to construct an explicit "cross" scheme using Ambartsumyan's theory, if tangential external forces on the face surfaces cannot be neglected. Obviously, this result is carried over to the more general case of thermoelastoplastic deformation of CM plates. Therefore, in this study, we consider only partial cases of spatial structures of reinforcement and load of CM-structures, in which an explicit numerical scheme of the "cross" type can be used. Further, we assume: a particular, but practically important case of loading of a plate, when external tangential forces on the face surfaces can be neglected, is investigated; the structure of spatial reinforcement has a following property: if a fiber of a certain family has an oblique direction $0 < \theta_k < \pi/2$ (see (41)[1] and Fig. 2), then there will certainly be another family of oblique fibers with reinforcement parameters $\theta_m = \pi - \theta_k$, $\varphi_m = \varphi_k$, $\omega_m = \omega_k$, $1 \le k$, $m \le N$, $m \ne k$, made from the same material as fibers of the k-th family. Structures with such a feature of reinforcement are often encountered in practice [17]. In particular, these include the reinforcement structure shown in Fig. 1***b***, as well as structures with orthogonal spatial reinforcement [8, 19] or structures with plane criss-cross reinforcement (Fig. 1***a***).

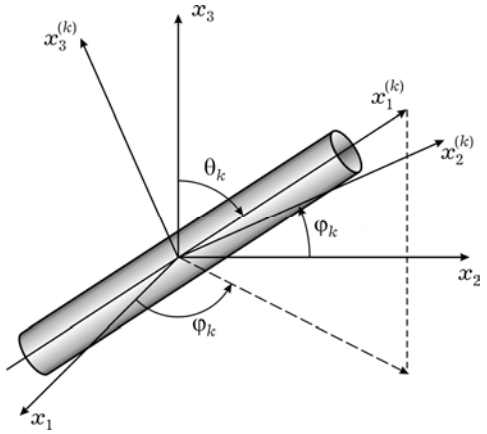

Fig. 2. Local coordinate system connected with a fibre of the k-th family.

[1] In the present work, for the sake of convenience, we continue the enumeration of formulas originated in [24].

According to this remark, in the framework of Ambartsumian's theory, the averaged strains ε_{ij} of the composition and displacement of points U_i of the CM-plate are approximated by the formulas [2, 20, 23]:

$$\varepsilon_{ij}(t,\mathbf{r}) = \frac{1}{2}(\partial_i u_j + \partial_j u_i) - x_3\partial_i\partial_j w + \frac{x_3}{3h^2}(3h^2 - x_3^2)(\partial_i\varepsilon_{j3}^0 + \partial_j\varepsilon_{i3}^0) + \\ + \frac{1}{2}\partial_i w\partial_j w,$$

$$\varepsilon_{i3}(t,\mathbf{r}) = \frac{h^2 - x_3^2}{h^2}\varepsilon_{i3}^0(t,\mathbf{x}), \quad \mathbf{x} = \{x_1, x_2\}, \quad \mathbf{r} = \{x_1, x_2, x_3\}, \ i,j = 1,2, \quad (51)$$

$$U_i(t,\mathbf{r}) = u_i(t,\mathbf{x}) - x_3\partial_i w + \frac{2x_3}{3h^2}(3h^2 - x_3^2)\varepsilon_{i3}^0,$$

$$U_3(t,\mathbf{r}) = w(t,\mathbf{x}), \quad \mathbf{x} \in \Omega, \quad |x_3| \le h, \quad t \ge t_0, \quad i = 1,2, \quad (52)$$

where u_i are displacements of points of the reference plane ($x_3 = 0$) in tangential directions x_i; w is deflection; ε_{i3}^0 denotes a deformation of transverse shears at points of the reference plane; ∂_i is operator of partial differentiation with respect to coordinate x_i; Ω is the domain occupied by the structure in the plan; t_0 denotes the initial moment of time t. In equalities (51) and (52), the functions u_i, w and ε_{i3}^0, $i = 1,2$, are unknown.

In this work, the mechanical behavior of a CM-plate as a flexible thin-walled system is simulated. Therefore, the transverse normal stress $\sigma_{33}(t,\mathbf{r})$ with an accuracy acceptable for practical applications can be approximated as follows [6]:

$$\sigma_{33}(t,\mathbf{r}) \equiv \sigma_3(t,\mathbf{r}) = \frac{\sigma_{33}^{(+)}(t,\mathbf{x}) - \sigma_{33}^{(-)}(t,\mathbf{x})}{2h}x_3 + \frac{\sigma_{33}^{(+)}(t,\mathbf{x}) + \sigma_{33}^{(-)}(t,\mathbf{x})}{2},$$

$$\mathbf{x} \in \Omega, \quad |x_3| \le h, \quad t \ge t_0, \quad (53)$$

where $\sigma_{33}^{(\pm)}(t,\mathbf{x}) \equiv \sigma_{33}(t,\mathbf{x},\pm h)$ are the normal stresses on the lower (−) and upper (+) face planes, which are known from the force boundary conditions.

Constitutive matrix equation (37) is a system of six algebraic equations. According to correspondence relations, similar to (30), from the third equation of this system at a discrete time t_n we determine the rate of transverse linear deformation of the composition:

$$\dot{\varepsilon}_{33}^{\,n} \equiv \dot{\varepsilon}_3^{\,n} = \frac{1}{b_{33}^{\,n}}\left(\dot{\sigma}_3^{\,n} - \sum_{i=1}^{6}(1-\delta_{3i})\,b_{3i}^{\,n}\,\dot{\varepsilon}_i^{\,n} - p_3^{\,n}\right), \quad (54)$$

where b_{3i}, p_3, $i = 1,2,\ldots,6$, are the elements of the matrix $\mathbf{B}$ and the column vector $\mathbf{p}$ in equality (37); the derivative $\dot{\sigma}_3$ is known from (53) after differentiation with respect to t. The strain rates $\dot{\varepsilon}_i$ on the right-hand side of equality (54) are obtained after differentiation of equalities (51) with respect to time, i.e. they are expressed in terms of two-dimensional functions w, $\dot{w}$, $\dot{u}_\ell$ and $\dot{\varepsilon}_{\ell 3}^0$, $\ell = 1,2$.

The kinematic relations (51) and (52) should be supplemented by two-dimensional equations of motion of the flexible plate and the corresponding initial and boundary conditions, which are commonly known [2, 23], so we will not present them here (see equalities (25)−(29) in [20]).

If the mechanical and thermophysical problems of thermoelastoplastic deformation of reinforced plates are coupled, it is additionally necessary to use the heat balance equation for CM [7, 9]:

$$\rho c\dot{\Theta} = -\operatorname{div}\mathbf{q} + \bar{w}(t,\mathbf{r}), \tag{55}$$

where

$$\rho \equiv \sum_{k=0}^{N} \omega_k \rho_k, \qquad c \equiv \frac{1}{\rho}\sum_{k=0}^{N} \omega_k c_k \rho_k, \qquad \bar{w}(t,\mathbf{r}) \equiv \sigma_{ij}\dot{\varepsilon}_{ij}, \tag{56}$$

ρ_k, ρ is the volumetric density of the k-th component of the composition and CM; c_k, c is the specific heat of the same materials; $\bar{w}$ denotes a power density of mechanical dissipation of CM; $\mathbf{q}$ is the averaged vector of the heat flux in the composition; σ_{ij}, ε_{ij} are averaged stresses and strains in the CM; Θ is a temperature of CM; the overdot denotes the operation of differentiation with respect to time t; the quantity ω_0 is defined in (38). The relationship between $\mathbf{q}$ and Θ is given by the Fourier law (see matrix equality (48) with regard for (49) and (50)).

We assume that on the face surfaces of the plate the combinations of heat boundary conditions of the second and third kind are specified [11]:

$$q_3^{(+)}(t,\mathbf{x}) \equiv q_3(t,\mathbf{x},h) = \alpha^{(+)}\left(\Theta - \Theta_\infty^{(+)}\right)\Big|_{x_3=h} + q_\infty^{(+)}(t,\mathbf{x}),$$

$$q_3^{(-)}(t,\mathbf{x}) \equiv q_3(t,\mathbf{x},-h) = -\alpha^{(-)}\left(\Theta - \Theta_\infty^{(-)}\right)\Big|_{x_3=-h} + q_\infty^{(-)}(t,\mathbf{x}), \quad \mathbf{x}\in\Omega,\ t\ge t_0, \tag{57}$$

where $\alpha^{(\pm)}$ are the coefficients of heat transfer from the side of the upper (+) and lower (−) face planes; $\Theta_\infty^{(\pm)}$ are ambient temperatures from the side of the same surfaces; $q_\infty^{(\pm)}$ are given projections onto the axis Ox_3 of external heat fluxes through the same surfaces.

On the end face the general heat boundary conditions can be specified

$$q_1 n_1 + q_2 n_2 = \alpha_*\left(\Theta - \Theta_\infty^*\right) + q_\infty^*(t,\mathbf{r}), \qquad \mathbf{x}\in\Gamma, \qquad |x_3| \le h, \qquad t \ge t_0,$$

$$n_1 = \cos\beta, \qquad n_2 = \sin\beta, \tag{58}$$

where α_*, Θ_∞^*, q_∞^* have the same meaning as similar values in (57), only on the end face; Γ is a contour that bounds the domain Ω; β denotes the angle that specifies the direction of the outer normal to Γ. In equalities (57) and (58), q_i, $i = 1,2,3$, are the components of the vector $\mathbf{q}$ (see (49)). In addition to boundary conditions (57) and (58), at the moment of time t_0, it is necessary to prescribe the initial condition for the temperature Θ.

To reduce the dimension of Eq. (55), we approximate the temperature Θ of a plate by a polynomial of the M-th degree in the transverse coordinate x_3:

$$\Theta(t,\mathbf{r}) - \Theta^0 = \sum_{\ell=0}^{M} \Theta_\ell(t,\mathbf{x}) x_3^\ell, \qquad \mathbf{x}\in\Omega, \qquad |x_3| \le h, \qquad t \ge t_0, \tag{59}$$

where Θ_ℓ, $0 \le \ell \le M$, are the required two-dimensional functions; $\Theta^0 = \text{const}$ is a temperature of the natural state of the CM-structure. For $M = 2$, we obtain the simplest version of the method of additional boundary conditions [12].

According to the remark made, for the considered structures of

reinforcement, the axis Ox_3 coincides with one of the principal directions of the thermophysical anisotropy of the CM, therefore

$$\lambda_{3i} = \lambda_{i3} \equiv 0, \qquad i = 1,2, \tag{60}$$

where λ_{ij} are the effective coefficients of thermal conductivity of the composition (elements of the 3×3-matrix $\mathbf{\Lambda}$ in (48) and (49)).

Substituting the expansions (59) into equalities (57) and using Fourier's law (48) with regard to (60), after elementary transformations we obtain

$$-\sum_{\ell=0}^{M}(-1)^{\ell}h^{\ell-1}\left(\ell\lambda_{33}^{(-)}+h\alpha^{(-)}\right)\Theta_{\ell}(t,\mathbf{x}) = \alpha^{(-)}\left(\Theta_{\infty}^{(-)}-\Theta^{0}\right)+q_{\infty}^{(-)}(t,\mathbf{x}),$$

$$\sum_{\ell=0}^{M}h^{\ell-1}\left(\ell\lambda_{33}^{(+)}+h\alpha^{(+)}\right)\Theta_{\ell}(t,\mathbf{x}) = \alpha^{(+)}\left(\Theta_{\infty}^{(+)}-\Theta^{0}\right)-q_{\infty}^{(+)}(t,\mathbf{x}),$$

$$\mathbf{x}\in\Omega, \quad t\ge t_0, \tag{61}$$

where

$$\lambda_{33}^{(\pm)} \equiv \lambda_{33}\big|_{\Theta=\Theta(t,\mathbf{x},\pm h)}, \tag{62}$$

$\lambda_{33}^{(\pm)}$ are coefficients of transverse thermal conductivity of CM on the upper (+) and lower (−) face surfaces. Relation (62) is true in the case of the thermal sensitivity of the coefficient $\lambda_{33}=\lambda_{33}(\mathbf{x};\Theta)$, in the opposite case $\lambda_{33}^{(+)}=\lambda_{33}^{(-)}=\lambda_{33}(\mathbf{x})$, in view of the homogeneity of the reinforcement structure across the thickness of the plate.

The system of two equations (61) with regard for (60) and (62), contains $M+1$ unknown two-dimensional functions $\Theta_{\ell}(t,\mathbf{x})$, $0\le\ell\le M$. To close this system, we will use the generalized Galerkin method, i.e. we integrate the heat balance equation (55) over the thickness of the plate with weights x_3^m, $0\le m\le M-2$, then we obtain

$$\rho\dot{U}^{(m)} = -\partial_1 Q_1^{(m)} - \partial_2 Q_2^{(m)} - \bar{Q}_3^{(m)} + W^{(m)}(t,\mathbf{x}),$$

$$\mathbf{x}\in\Omega, \quad t\ge t_0, \quad 0\le m\le M-2, \tag{63}$$

where

$$U^{(m)}(t,\mathbf{x}) \equiv \int_{-h}^{h} U(t,\mathbf{r})x_3^m\,dx_3,$$

$$\bar{Q}_3^{(m)}(t,\mathbf{x}) \equiv \int_{-h}^{h}\partial_3 q_3(t,\mathbf{r})\,x_3^m\,dx_3 = q_3(t,\mathbf{r})x_3^m\Big|_{-h}^{h} - m\int_{-h}^{h} q_3(t,\mathbf{r})x_3^{m-1}\,dx_3 =$$

$$= h^m\left[q_3^{(+)}-(-1)^m q_3^{(-)}\right] - mQ_3^{(m-1)}(t,\mathbf{x}),$$

$$Q_i^{(m)}(t,\mathbf{x}) \equiv \int_{-h}^{h} q_i(t,\mathbf{r})x_3^m\,dx_3, \qquad i=1,2,3,$$

$$W^{(m)}(t,\mathbf{x}) \equiv \int_{-h}^{h}\bar{w}(t,\mathbf{r})x_3^m\,dx_3, \qquad \frac{\partial U}{\partial\Theta}=c(\Theta), \tag{64}$$

U is the specific internal energy of the CM.

The analysis of experimental data shows [3, 14] that with an accuracy acceptable for practical applications in a sufficiently wide temperature range, the heat capacity of the k-th component of the composition c_k can be approximated by a square parabola of the difference $\Theta-\Theta^0$ (more complex depen-

dencies $c_k(\Theta - \Theta^0)$ can also be used, this is not essential). Then, according to the second equality (56), the specific heat capacity of the composition in the case of taking into account the thermal sensitivity can be represented in the form

$$c(\mathbf{x}; \Theta - \Theta^0) = C_0(\mathbf{x}) + C_1(\mathbf{x})(\Theta - \Theta^0) + C_2(\mathbf{x})(\Theta - \Theta^0)^2, \quad \mathbf{x} \in \Omega, \tag{65}$$

where

$$C_i(\mathbf{x}) \equiv \frac{1}{\rho} \sum_{k=0}^{N} c_i^{(k)} \rho_k \omega_k(\mathbf{x}), \qquad i = 0, 1, 2, \tag{66}$$

$c_i^{(k)}$ are the expansion coefficients of the specific heat capacity of the k-th component of the composition $c_k(\Theta - \Theta^0)$ according to a formula analogous to (65).

From the last formula (64), taking into account (65) and (66), we obtain

$$U(\mathbf{x}; \Theta - \Theta^0) = U_0 + C_0(\mathbf{x})(\Theta - \Theta^0) + \frac{C_1(\mathbf{x})}{2}(\Theta - \Theta^0)^2 + \frac{C_2(\mathbf{x})}{3}(\Theta - \Theta^0)^3, \tag{67}$$

where U_0 is a value independent of temperature. Since the temperature Θ of CM is of interest below, and not the internal energy U, the value U_0 corresponding to the temperature Θ^0 can be given arbitrarily, for example, for convenience, equals to zero.

After substitution (67) into the first equality (64), with regard for the expansion (59), we obtain

$$C_0 \sum_{i=0}^{M} H(i+m)\Theta_i + \frac{C_1}{2} \sum_{i=0}^{M} \sum_{j=0}^{M} H(i+j+m)\Theta_i\Theta_j + \frac{C_2}{3} \sum_{i=0}^{M} \sum_{j=0}^{M} \sum_{\ell=0}^{M} H(i+j+\ell+m)\Theta_i\Theta_j\Theta_\ell = U^{(m)}(t, \mathbf{x}),$$

$$\mathbf{x} \in \Omega, \quad t \geq t_0, \quad 0 \leq m \leq M-2, \tag{68}$$

where

$$H(s) \equiv \frac{h^{s+1}}{s+1}\left[1 - (-1)^{s+1}\right]. \tag{69}$$

If at the current moment of time t from any reasonings the values of the functions $U^{(m)}$ are known, then the system of nonlinear (in the case of accounting the thermal sensitivity) equations (61) and (68) with regard for (62) and (69) will be closed with respect to the functions $\Theta_\ell(t, \mathbf{x})$, $0 \leq \ell \leq M$.

To obtain the boundary conditions corresponding to the two-dimensional heat balance equations (63), it is necessary to integrate equality (58) over the thickness of the plate with weights x_3^m. Then, taking into account notations (64) and expansion (59), we obtain

$$Q_1^{(m)} n_1 + Q_2^{(m)} n_2 - \alpha_* \sum_{\ell=0}^{M} H(\ell+m)\Theta_\ell = -\alpha_* H(m)(\Theta_\infty^* - \Theta^0) + Q_\infty^{(m)}(t, \mathbf{x}),$$

$$\mathbf{x} \in \Gamma, \qquad t \geq t_0, \qquad 0 \leq m \leq M-2, \tag{70}$$

where

$$Q_\infty^{(m)}(t, \mathbf{x}) \equiv \int_{-h}^{h} q_\infty^*(t, \mathbf{r})\, x_3^m \, dx_3, \qquad 0 \leq m \leq M-2. \tag{71}$$

The initial condition for equation (63) has the form

$$U^{(m)}(t_0,\mathbf{x}) = U_0^{(m)}(\mathbf{x}), \qquad \mathbf{x}\in\Omega, \qquad 0\le m\le M-2, \tag{72}$$

where $U_0^{(m)}$ are the known two-dimensional functions, which are calculated by the first formula in (64) with regard to the expression (67), where it is necessary to replace Θ by the known initial temperature $\Theta_0^*(\mathbf{r})$ of the plate.

From the closed system of two-dimensional equations (61), (63), in view of (64), (68), we obtain that the number M in the temperature expansion (59) should be at least two ($M\ge 2$) if the thermal boundary conditions on the face surfaces of the plate are taken into account (see (61)).

2. Method of calculation. As noted in the Introduction and in [24], to integrate the problem we will use explicit step-by-step numerical schemes, determining the solution at discrete times t_n, $n=0,1,2,\ldots$. In this connection, we assume that, for $t=t_m$, in addition to (32), the values of the following functions are already known:

$$\overset{m}{u}_\ell(\mathbf{x})\equiv u_\ell(t_m,\mathbf{x}),\quad \overset{m}{w}(\mathbf{x})\equiv w(t_m,\mathbf{x}),\quad \overset{m}{\gamma}_\ell(\mathbf{x})\equiv\gamma_\ell(t_m,\mathbf{x}),\quad \overset{m}{\sigma}_{ij}(\mathbf{r})\equiv\sigma_{ij}(t_m,\mathbf{r}),$$

$$\overset{m}{\sigma}{}_{33}^{(\pm)}(\mathbf{x})\equiv\sigma_{33}^{(\pm)}(t_m,\mathbf{x}),\quad \overset{n}{U}{}^{(r)}(\mathbf{x})\equiv U^{(r)}(t_n,\mathbf{x}),\quad \overset{n}{q}_i(\mathbf{r})\equiv q_i(t_n,\mathbf{r}),$$

$$\overset{n}{\Theta}_s(\mathbf{x})\equiv\Theta_s(t_n,\mathbf{x}),\quad \overset{n}{q}{}_\infty^{(\pm)}(\mathbf{x})\equiv q_\infty^{(\pm)}(t_n,\mathbf{x}),\quad \overset{m}{\sigma}{}_{ij}^{(k)}(\mathbf{r})\equiv\sigma_{ij}^{(k)}(t_m,\mathbf{r}),$$

$$\overset{m}{\varepsilon}{}_{ij}^{(k)}(\mathbf{r})\equiv\varepsilon_{ij}^{(k)}(t_m,\mathbf{r}),\quad \overset{m}{\chi}{}^{(k)}(\mathbf{r})\equiv\chi^{(k)}(t_m,\mathbf{r}),\quad \ell=1,2,\quad i,j=1,2,3,\quad 0\le k\le N,$$

$$m=n-1,n,\quad 0\le r\le M-2,\quad 0\le s\le M,\quad \mathbf{x}\in\Omega,\quad |x_3|\le h, \tag{73}$$

where

$$\gamma_i(t,\mathbf{x})\equiv\frac{8}{5}\varepsilon_{i3}^0-\partial_i w,\qquad i=1,2, \tag{74}$$

are functions introduced for the convenience of presentation [20].

The derivatives with respect to time in the mechanical component of the investigated coupled thermoelastoplastic problem will be approximated by central finite differences on a three-point template $\{t_{n-1},t_n,t_{n+1}\}$, which enables us to develop an explicit numerical scheme. Replacing the second time derivatives of the kinematic variables u_i and γ_i in the equations of motion of a flexible CM-plate by their finite-difference analogs and taking into account (52) and notations similar to (73), we obtain [20]

$$\frac{2h\rho}{\Delta^2}\left(\overset{n+1}{w}-2\overset{n}{w}+\overset{n-1}{w}\right)=\sum_{\ell=1}^{2}\partial_\ell\left(\overset{n}{F}_{\ell 3}+\sum_{j=1}^{2}\overset{n}{F}_{\ell j}\,\partial_j\overset{n}{w}\right)+\overset{n}{\sigma}{}_{33}^{(+)}-\overset{n}{\sigma}{}_{33}^{(-)},$$

$$\frac{2h\rho}{\Delta^2}\left(\overset{n+1}{u}_i-2\overset{n}{u}_i+\overset{n-1}{u}_i\right)=\sum_{j=1}^{2}\partial_j\left(\overset{n}{F}_{ij}-\overset{n}{F}_{j3}\,\partial_j\overset{n}{w}\right)-\left(\overset{n}{\sigma}{}_{33}^{(+)}-\overset{n}{\sigma}{}_{33}^{(-)}\right)\partial_i\overset{n}{w},$$

$$\frac{2h^3\rho}{3\Delta^2}\left(\overset{n+1}{\gamma}_i-2\overset{n}{\gamma}_i+\overset{n-1}{\gamma}_i\right)=\sum_{j=1}^{2}\partial_j\overset{n}{M}_{ij}-\overset{n}{F}_{i3},\quad i=1,2,\quad \mathbf{x}\in\Omega,\quad n=1,2,\ldots, \tag{75}$$

where

$$F_{ij}=\int_{-h}^{h}\sigma_{ij}\,dx_3,\quad F_{i3}=\int_{-h}^{h}\sigma_{i3}\,dx_3,\quad M_{ij}=\int_{-h}^{h}\sigma_{ij}x_3\,dx_3,\quad i,j=1,2, \tag{76}$$

Δ is a time step; the density ρ is determined in (56). The volumetric forces in the CM-plate are not taken into account.

Using (76) and assumptions (73) at a given time t_n, we can calculate all force factors F_{ij}, F_{i3}, M_{ij} and external loads $\sigma_{33}^{(\pm)}$ entered into the right-hand sides of equalities (75). Hence, taking into account the corresponding boundary conditions [20], the values of the unknown functions $\overset{n+1}{w}$, $\overset{n+1}{u_i}$, $\overset{n+1}{\gamma_i}$ at the next moment of time t_{n+1}, can be calculate from equations (75) by explicit scheme. Then, using formulas (51), taking into account (74), we determine the averaged deformations $\overset{n+1}{\varepsilon_{ij}}$ of the composition.

According to (51) and (73), the deformations $\overset{n-1}{\varepsilon_{ij}}$ are already known at $t = t_{n-1}$, therefore, based on the formulas of numerical differentiation with respect to t, using formulas (54), we can also calculate the strain rates $\overset{n}{\dot{\varepsilon}_{ij}}$ at each point of the plate at the time t_n.

Further, by formulas (42), taking into account the relations (30), we determine the deformation rates $\overset{n}{\dot{\boldsymbol{\varepsilon}}_k}$ of the components of the composition, and from relations (35), taking into account (36), we determine the stress rates $\overset{n}{\dot{\boldsymbol{\sigma}}_k}$.

Using approximations (43) taking into account (73), we calculate the stresses $\overset{n+1}{\boldsymbol{\sigma}_k}$ and strains $\overset{n+1}{\boldsymbol{\varepsilon}_k}$ in the k-th component of the composition, then by formula (46), taking into account (44), (45), and (47), we determine the value of the Odquist parameter $\overset{n+1}{\chi^{(k)}}$ in the same material at the next moment of time t_{n+1}.

According to (31), the switching parameter $c^{(k)}$ at $t = t_n$ depends on $\overset{n}{\dot{\boldsymbol{\varepsilon}}_k}$, therefore, at the current instant t_n, the constitutive relation (35) (or (29)) must be iteratively refined using the method of variable parameters of elasticity [18]. The performed calculations show that in order to obtain an accuracy acceptable in practical applications, it is sufficient to use two iterations at each time step.

To integrate the thermophysical component of the problem under consideration, we will also use an explicit scheme, but on a two-point template in time $\{t_n, t_{n+1}\}$. Then the heat balance equations (63), taking into account the notations similar to (73), take the form [15]

$$\frac{\rho}{\Delta}\left(\overset{n+1}{U^{(m)}} - \overset{n}{U^{(m)}}\right) = -\partial_1 \overset{n}{Q_1^{(m)}} - \partial_2 \overset{n}{Q_1^{(m)}} - \overset{n}{\bar{Q}_3^{(m)}} + \overset{n}{W^{(m)}},$$

$$\mathbf{x} \in \Omega, \qquad 0 \le m \le M-2, \qquad n = 0, 1, 2, \ldots. \tag{77}$$

Based on formulas (64), taking into account assumptions (73), at the current moment of time t_n, we can calculate the right-hand side in (77), and then by explicit scheme, with regard for (70)–(73), we determine the values of the functions $\overset{n+1}{U^{(m)}}$ at the next moment of time t_{n+1}. Further, considering at

$t = t_{n+1}$ equations (61) and (68) (in which the right-hand sides are already known) and taking into account (62) and (69), we determine the expansion coefficients of temperature $\overset{n+1}{\Theta}_{\ell}(\mathbf{x})$, $0 \le \ell \le M$, in formula (59). If the thermal sensitivity of the materials of the composition is taken into account, system (61), (68) is nonlinear. For its linearization, can be used the method of variable thermophysical parameters, similar to the method of variable elasticity parameters [18]. Calculations have shown that for the convergence of such an iterative process with an accuracy acceptable for applications, it is sufficient to use two or three iterations.

According to the structure of the left-hand sides of equations (75) and (77), to start calculations by the proposed numerical scheme it is necessary preliminarily to know the functions $\overset{m}{w}$, $\overset{m}{u}_i$, $\overset{m}{\gamma}_i$, $m = 0,1$, and $\overset{0}{U}^{(\ell)}$. In this case, the functions $\overset{0}{w}$, $\overset{0}{u}_i$, $\overset{0}{\gamma}_i$ and $\overset{0}{U}^{(\ell)}$, $0 \le \ell \le M-2$, are determined from the initial conditions (see (72) and (28) in [20]). If at $t = t_0$ the CM-plate is at rest in the natural state and there are no external loads ($\overset{0}{\sigma}{}^{(+)}_{33} - \overset{0}{\sigma}{}^{(-)}_{33} = 0$), then using the Taylor formula we obtain $\overset{1}{w} \approx \overset{1}{u}_i \approx 0$, $\overset{1}{\gamma}_i \approx 0$, $i = 1,2$, accurate to within Δ^3.

Replacing derivatives $\partial_i(\bullet)$ in (75) and (77) by their finite-difference analogs and adding to these equations the necessary boundary conditions (see (70) and (71), as well as (29) in [20]), we finally obtain an explicit step-by-step scheme of the numerical integration of the coupled problem of thermoelastoplastic deformation of a flexible CM-plate.

3. Discussion of the calculation results. Let us investigate the thermoelastoplastic dynamic behavior of flexible plates with a thickness $2h = 2$ cm. The domain occupied by them in the plan is Ω: $|x_1| \le a/2$, $|x_2| \le b/2$, $a = 3b$. The edges of the structures are rigidly fixed: $w = u_i = 0$, $\gamma_i = 0$, $\mathbf{x} \in \Gamma$, $t \ge t_0$ (see (52), (74), (75)). Until the initial moment of time $t_0 = 0$, the plates are in the state of rest ($w = u_i = 0$, $\gamma_i = 0$, $\mathbf{x} \in \Omega$, $t = t_0$, $i = 1,2$) at the temperature of the natural state ($\Theta = \Theta^0 = \text{const}$, $\mathbf{x} \in \Omega$, $|x_3| \le h$, $t = t_0$). At the initial time $t = t_0$, the structure are loaded from below by the pressure $p(t)$ generated by the air blast wave [22]

$$\sigma^{(+)}_{33} \equiv 0, \qquad -\sigma^{(-)}_{33} \equiv p(t) = \begin{cases} p_{\max} t / t_{\max}, & 0 \le t \le t_{\max}, \\ p_{\max} \exp\left[-\alpha(t - t_{\max})\right], & t > t_{\max}, \end{cases} \tag{78}$$

where

$$\alpha = -\ln(0.01)/(t_{\min} - t_{\max}) > 0, \qquad t_{\min} \gg t_{\max}, \tag{79}$$

$t_{\max}$ is the moment of time when $p(t)$ reaches the largest value $p_{\max}$; $t_{\min}$ is the moment of time above which it can be neglected $p(t)$ in comparison with $p_{\max}$ (for example, formula (79) is valid for $p(t_{\min}) = 0.01\, p_{\max}$). Based on the experimental data [22], in the calculations we take $t_{\max} = 0.1$ ms and $t_{\min} = 2$ ms.

Through the face surfaces ($x_3 = \pm h$) convective heat exchange with the environment ($q^{(\pm)}_{\infty} \equiv 0$) occurs under conditions of natural convection

($\alpha^{(\pm)} = 30\ \mathrm{W/(m^2 \cdot K)}$ [13]) at an air temperature equals to the temperature of the natural state of structures: $\Theta_{\infty}^{(\pm)} = \Theta^0 = 20\ ^\circ\mathrm{C}$ (see (57)). Boundary conditions of the first kind are given on the end surfaces of the plates, and the temperature of the structures is maintained equal to the temperature of their natural state: $\alpha_* \to \infty$, $\Theta_{\infty}^{*} = \Theta^0$ (see (58)).

The plates are made of magnesium alloy VT65 [3] and reinforced with steel wire U8A [10] (metal composition) or epoxy binder [16] reinforced with glass fibers [10] (fiberglass). Elastoplastic deformation of the components of the composition under active loading and constant temperature Θ is described by a bilinear diagram

$$\sigma = \begin{cases} E^{(k)}\varepsilon, & |\varepsilon| \le \varepsilon_{\mathrm{s}}^{(k)} = \sigma_{\mathrm{s}}^{(k)}/E^{(k)}, \\ \operatorname{sgn}(\varepsilon)\sigma_{\mathrm{s}}^{(k)} + E_{\mathrm{s}}^{(k)}\left(\varepsilon - \operatorname{sgn}(\varepsilon)\varepsilon_{\mathrm{s}}^{(k)}\right), & |\varepsilon| > \varepsilon_{\mathrm{s}}^{(k)}, \quad 0 \le k \le N, \end{cases}$$

where σ, ε are axial stress and strain; $E_{\mathrm{s}}^{(k)} = E_{\mathrm{s}}^{(k)}(\Theta)$ is modulus of linear hardening of the material of the k-th component of the composition; $\sigma_{\mathrm{s}}^{(k)} = \sigma_{\mathrm{s}}^{(k)}(\Theta)$ is the yield point of the same component at a fixed temperature ($\Theta = \mathrm{const}$). The physical and mechanical characteristics of the materials of the composition are given in the Table 1, where $\overline{c} = \sqrt{E/\rho}$ is the speed of sound, $\overline{a} = 2\lambda/(c\rho)$ is the doubled thermal diffusivity, and in parentheses is indicated the temperature (Θ),°C, at which the value of the corresponding characteristic is determined. The dependences of all physical and mechanical characteristics on temperature Θ in the calculations were approximated linearly, according to the data presented in the Table 1.

To carry out calculations in spatial variables x_1 and x_2 a uniform grid $\Delta x_1 = \Delta x_2 = b/100$ was introduced, and the time step Δ was chosen equal to 0.25 μs. We considered relatively thin ($b = 1\ \mathrm{m}$, $2h/b = 1/50$) and relatively thick ($b = 20\ \mathrm{cm}$, $2h/b = 1/10$) CM-plates, for which

$$\frac{\Delta x_1}{\Delta} = 40\ \mathrm{km/s}, \quad \frac{2h}{\Delta} = 80\ \mathrm{km/s}, \quad \frac{(\Delta x_1)^2}{\Delta} = 400\ \mathrm{m^2/s} \quad \text{for} \quad b = 1\ \mathrm{m},$$

$$\frac{\Delta x_1}{\Delta} = 8\ \mathrm{km/s}, \quad \frac{2h}{\Delta} = 80\ \mathrm{km/s}, \quad \frac{(\Delta x_1)^2}{\Delta} = 16\ \mathrm{m^2/s} \quad \text{for} \quad b = 20\ \mathrm{m}. \qquad (80)$$

To ensure the stability of the explicit scheme (75), it is necessary to satisfy the Courant conditions: $\Delta x_1/\Delta \ge \overline{c}$ and $2h/\Delta \ge \overline{c}$ [1], and for the stability of the explicit scheme (77), it is necessary that $(\Delta x_1)^2/\Delta \ge \overline{a}$ [15]. According to the numerical data obtained in (80), these ratios significantly exceed the corresponding values for $\overline{c}$ and $\overline{a}$ for the components of the compositions presented in the Table 1. Hence, similar necessary conditions for the stability of the explicit scheme (75) and (77) will be fulfilled with a reserve for the considered compositions.

Note that scheme (77) has the first order of accuracy with respect to Δ [15], however, the smallness of the time step ($\Delta = 0.25$ μs), which guarantees the stability of the entire numerical scheme as a whole (see (75) and (77)), provides a quite acceptable for practical applications accuracy of calculation.

Reinforcement structures of CM-plates are homogeneous: $\theta_k = \mathrm{const}$, $\varphi_k = \mathrm{const}$, $\omega_k = \mathrm{const}$, $1 \le k \le N$ (see (38), (41), (49) and Fig. 2). Two schemes of reinforcement are considered: ***1***) plane orthogonal reinforcement (Fig. 1***a***), when two ($N = 2$) families of fibers are laid in directions x_1 and x_2 with densities of reinforcement $\omega_1 = 0.1$ and $\omega_2 = 0.3$, respectively; ***2***) spatial

reinforcement in four ($N = 4$) directions (Fig. 1***b***), when the first two families of fibers are still laid in the directions x_1 and x_2, and the third and fourth ones are oblique in the plane Ox_2x_3 along the directions that are specified by the angles (see (41) and Fig. 2): $\theta_3 = \pi/4$, $\theta_4 = 3\pi/4$, $\varphi_3 = \varphi_4 = \pi/2$ (in Fig. 1***b*** angle $\theta = \pi/4$). In the second structure, the densities of reinforcement are as follows: $\omega_1 = 0.1$, $\omega_2 = 0.2$, $\omega_3 = \omega_4 = 0.05$. In both schemes of reinforcement, the total fiber consumption is the same.

Table 1. Physico-mechanical characteristics of material components [3, 10, 16].

Characteristic of material	Epoxy resin	Glass-fibres material	Magnesium alloy VT65	Still wire U8A
ρ, kg/m^3	1210.0 (20)	2520.0 (20)	1800.0 (20)	7800.0 (20)
	1208.0 (40)	2519.6 (80)	1796.2 (100)	7791.8 (100)
E, GPa	2.8 (20)	86.8 (20)	43.0 (20)	210.0 (20)
	2.3 (40)	86.3 (80)	38.5 (100)	195.0 (100)
ν	0.33 (20)	0.25 (20)	0.330 (20)	0.3 (20)
	0.333 (40)	0.254 (80)	0.334 (100)	0.305 (100)
σ_s, MPa	20 (20)	4500 (20)	267 (20)	3968 (20)
	18 (40)	4400 (80)	219 (100)	3971 (200)
E_s, GPa	1.114 (20)	6.230 (20)	0.379 (20)	6.973 (20)
	0.783 (40)	5.168 (80)	0.367 (100)	5.014 (200)
λ, W/(m · K^{-1})	0.243 (20)	0.89 (20)	117.23 (20)	42.7 (20)
	0.240 (40)	0.86 (80)	121.42 (100)	41.7 (100)
$\alpha \cdot 10^6$, K^{-1}	68.1 (20)	2.5 (20)	20.9 (20)	12.3 (20)
	70.3 (40)	2.6 (80)	22.6 (100)	13.2 (100)
c, kJ/(kg · K)	1.54 (20)	0.800 (20)	1.032 (20)	0.485 (20)
	1.60 (40)	0.839 (80)	1.054 (100)	0.488 (100)
$\overline{c}$, m/c	1521 (20)	5869 (20)	4888 (20)	5189 (20)
	1380 (40)	5852 (80)	4635 (100)	5003 (100)
$\overline{a}$, m^2/c	$2.60 \cdot 10^{-7}$ (20)	$8.80 \cdot 10^{-7}$ (20)	$1.27 \cdot 10^{-4}$ (20)	$2.26 \cdot 10^{-5}$ (20)
	$2.48 \cdot 10^{-7}$ (40)	$8.14 \cdot 10^{-7}$ (80)	$1.29 \cdot 10^{-4}$ (100	$2.19 \cdot 10^{-5}$ (100)

In order to clarify the question of choosing the value M in expansion (59), at which an acceptable accuracy of calculations of temperature Θ is ensured, the dependences of the maximum values $\Theta_{\max}(M) = \max\limits_{t,\mathbf{r}} \Theta(t, \mathbf{r}; M)$ on M were investigated ($|x_1| \le a/2$, $|x_2| \le b/2$, $|x_3| \le h$, calculations were carried out over a time interval $0 \le t \le 0.1$ s). In Fig. 3 shows the graphs of these dependences for relatively thin ($b = 1$ m): fiberglass plates (curves ***1*** and ***2***), calculated at $p_{\max} = 4$ MPa (see (78)), and metal-composite structures at $p_{\max} = 10$ MPa (curves ***1′*** and ***2′***); and also for relatively thick ($b = 20$ cm) fiberglass plates at $p_{\max} = 7$ MPa (curves ***1″*** and ***2″***). At such loading levels of CM-structures, plastic deformations arise in them. The value $M = 0$ in Fig. 3 conditionally corresponds to the case of complete neglect of the thermal effect, therefore it is assumed that $\Theta_{\max} = \Theta^0 = 20\,^\circ$C for $M = 0$. The numbers of the curves in Fig. 3 coincide with the numbers of the structures of reinforcement.

The behavior of all curves in Fig. 3 demonstrates that in passing from value $M = 6$ to value $M = 7$, the increment of value Θ_{max} is practically negligible. At values $M \geq 8$, the linearized system of equations (61), (68) (with taking into account (69)), from which the temperature expansion coefficients (59) are calculated at a given time, becomes ill-conditioned. Therefore, the dependences $\Theta_{max}(M)$ at $M \geq 8$ diverge, and the corresponding segments of the curves in Fig. 3 are not shown.

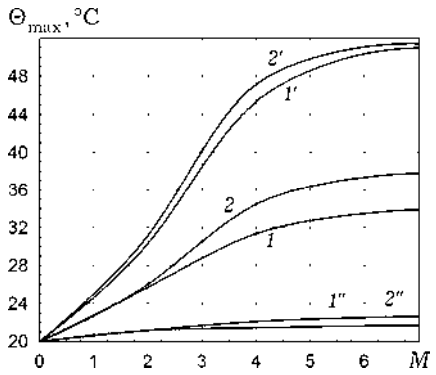

Fig. 3. Dependence of the maximum value of temperature on the order of its approximating polynomial in transverse direction.

When carrying out practical calculations, it is generally accepted that it is quite sufficient to approximate the temperature across the thickness of thin-walled structures linearly ($M = 1$) or with a square parabola ($M = 2$). Comparison of the ordinates of the points on the curves in Fig. 3 for values $M = 1$ or $M = 2$ and for $M = 7$ indicates that in cases of elastoplastic dynamic deformation of flexible CM-plates, the linear and quadratic temperature distribution in the transverse direction in them leads to a significant underestimation of the largest calculated temperature values. Hence, in order to carry out adequate calculations of the temperature fields under such deformation of thin-walled CM-structures, it is advisable to approximate the temperature along their thickness by polynomials of the 6th or 7th orders (see (59) for $M = 6$ or $M = 7$).

To obtain a more visual representation of the difference between the temperature fields calculated in the considered CM-plates for $M = 2$ and $M = 7$, in Fig. 4 shows the oscillations of the maximum values of temperature $\Theta_m(t; M) = \max_{\mathbf{r}} \Theta(t, \mathbf{r}; M)$ as a function of time t. The curves in Fig. 4***a*** are calculated for thin fiberglass structures, in Fig. 4***b*** – for relatively thick fiberglass plates, and in Fig. 4***c*** – for relatively thin metal-composite structures. In order not to clutter up the Fig. 4, it shows the dependences $\Theta_m(t; M)$ only for CM-plates with 2D-structures of reinforcement. Here, solid curves ***1*** correspond to the case $M = 2$, and dashed lines ***2*** correspond to the case $M = 7$. Comparison of the behavior of curves ***1*** and ***2*** in Fig. 4 demonstrates the fact that the calculation of the dependence $\Theta_m(t; M)$ with the simplest (quadratic, $M = 2$) approximation of temperature only qualitatively (and very approximately), but not quantitatively, enable us to calculate the oscillations of the largest values Θ in the considered CM-structures.

The behavior of the curves in Fig. 4***a*** and Fig. 4***c*** indicates that the maximum values of the temperature in relatively thin CM-plates are achieved at times (in Fig. 4***a*** at $t \approx 63$ ms, and in Fig. 4***c*** at $t \approx 25$ ms), which are much larger than the time of action of an external short-term load, i.e. much larger than $t_{min} = 2$ ms (see (79)). The behavior of the curves in Fig. 4***b*** shows that in the case of relatively thick fiberglass structures, the dependences $\Theta_m(t; M)$ at different values M reach their maximum values at the first oscillation, i.e. at times (in Fig. 4***b*** at $t = 0.3$ ms) close to $t_{max} = 0.1$ ms (see (78)). A qualitatively similar behavior of the dependences of $\Theta_m(t; M)$ at the values $M = 2$ and $M = 7$ also takes place in the case of relatively thick metal-composite plates (at $p_{max} = 50$ MPa); therefore, the corresponding curves in Fig. 4 are not shown.

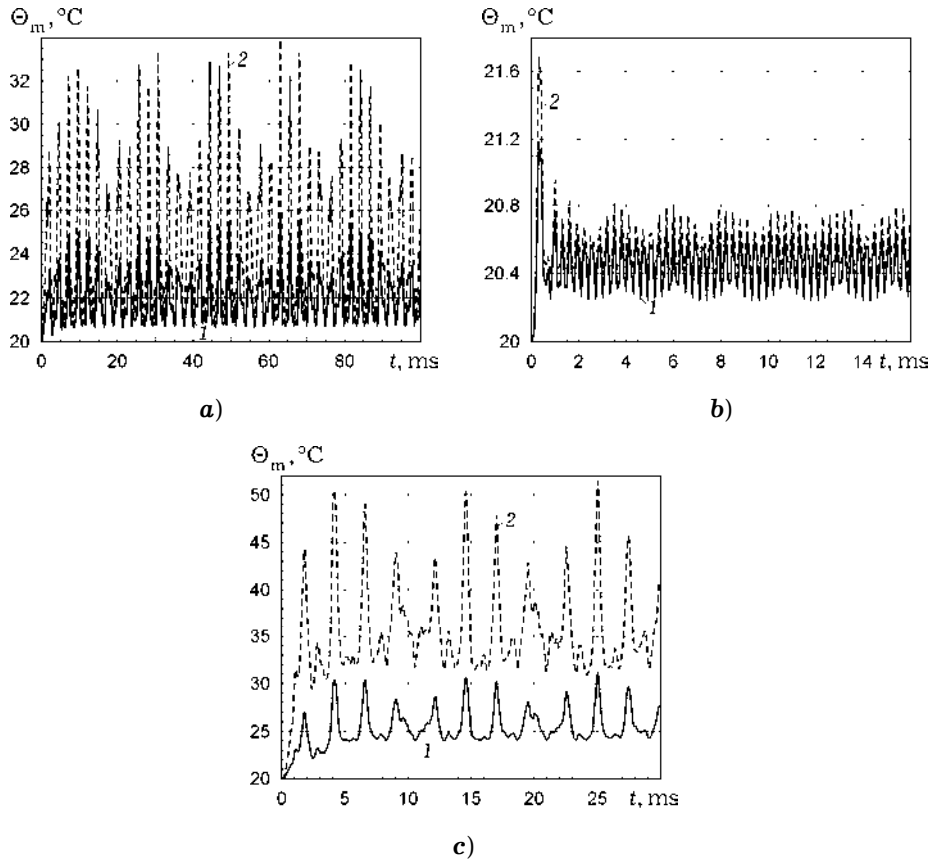

Fig. 4. Time dependences of the highest temperature values: ***a***) in a relatively thin fiberglass plates, ***b***) in a relatively thick fiberglass plates, and ***c***) in a relatively thin metal-composite structures, calculated using different approximations of the temperature field in the transverse direction.

In Fig. 5 are shown the oscillations of the highest values of the deformation intensity $\varepsilon_*^{(0)}$ of the binder of the investigated compositions ($\varepsilon_{\rm m}^{(0)}(t) = \max\limits_{\mathbf{r}} \varepsilon_*^{(0)}(t,\mathbf{r})$, $|x_1| \le a/2$, $|x_2| \le b/2$, $|x_3| \le h$). The curves in Fig. 5***a*** – Fig. 5***c*** are calculated for the same CM-structures as in Fig. 4***a*** – Fig. 4***c***, respectively. The numbers of the curves in Fig. 5 coincide with the numbers of the structures of reinforcement, as in Fig. 3. All curves in Fig. 5 (except for curve ***2′*** in Fig. 5***d***) were calculated for the value $M = 7$ (see (59)).

Comparison of curves ***1*** and ***2*** in Fig. 5***a*** and Fig. 5***c*** reveals that in relatively thin fiberglass and metal-composite plates, replacing the traditional 2D-structure of reinforcement (see Fig. 1***a***) with the spatial structure of 4D-reinforcement (see Fig. 1***b***) is ineffective, as if it leads to an increase of the highest values of deformations of the composition components. The behavior of the curves in Fig. 5***b*** indicates that, in relatively thick fiberglass structures, such a replacement of structures of reinforcement enable us to reduce the maximum values of the intensity of deformations of the binder material by two times. Though, at the same time, according to the behavior of curves ***1″*** and ***2″*** in Fig. 3 for $M = 7$, a structure with a 4D-structure of reinforcement heats up a little more than a plate with a 2D-structure. However, the difference in values is insignificant and is less than 1°C.

Additional calculations showed that, in relatively thick metal-composite plates (at $p_{\max} = 50$ MPa), the indicated replacement of the reinforcement

structure is also ineffective. This is explained by the fact that a relatively "rigid" metal binder resists lateral shears quite well even in thick metal-composite structures with a traditional 2D reinforcement structure.

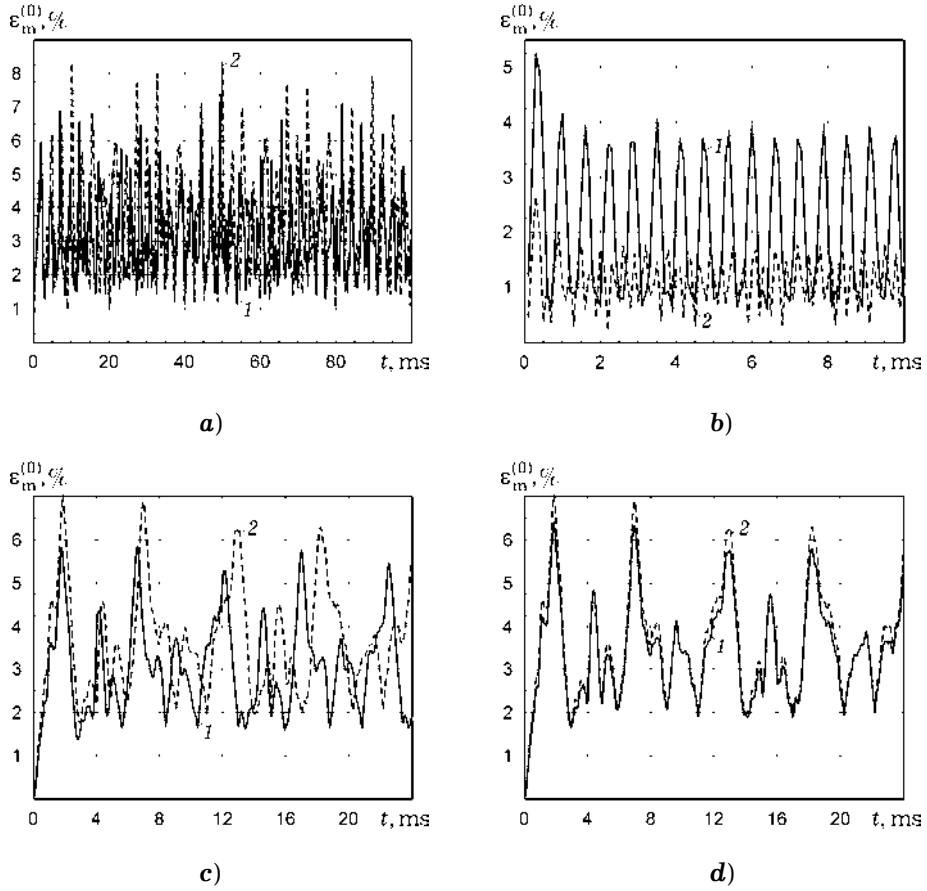

Fig. 5. Time dependences of the maximum value of the intensity of deformation of a binder: ***a***) in a relatively thin fiberglass plates, ***b***) in a relatively thick fiberglass plates, and ***c***), ***d***) in a relatively thin metal-composite structures with 2D- and 4D-reinforcement structures, respectively.

Curves ***2***, ***2′***, and ***2″*** in Fig. 3 lie above curves ***1***, ***1′***, and ***1″***, respectively. Hence, in all the cases considered above, replacing a 2D-reinforcement structure with a 4D-structure leads to an increasing the maximum values of temperature in the structure. This is especially pronounced in relatively thin fiberglass plates (see curves ***1*** and ***2*** in Fig. 3). It was noted in [19] that if the thermal conductivity of fibers is much greater than the analogous value of the binder, as is the case in fiberglass composites (see Table 1), then the use of spatial structures of reinforcement should contribute to more efficient heat removal from a thin-walled structure in comparison with traditional plane criss-cross structures. The behavior of the curves in Fig. 3 indicates that in the case of dynamic inelastic deformation of plates, replacing the 2D-structure of reinforcement with a 4D-structure does not contribute to more active heat removal from such CM structures.

The behavior of the curves in Fig. 4***a*** – Fig. 4***c*** and Fig. 5***a*** – Fig. 5***c*** is qualitatively similar. Namely, in Fig. 5***b***, the maximum value of the dependence $\varepsilon_m^{(0)}(t)$ is reached at the first oscillation at $t \approx 0.3$ ms; similarly in Fig. 4***b***, the maximum value of the dependence $\Theta_m(t)$ is reached at the first oscillation at the same time instant, i.e. approximately when the external load

reaches its highest value (see (78) and (79)). The maximum values of the quantities Θ_m and $\varepsilon_m^{(0)}$ in Fig. 4***a***, Fig. 4***c***, Fig. 5***a*** and Fig. 5***c*** are reached at times significantly exceeding $t_{\min} = 2$ ms, i.e. after the termination of the external short-time load. In this case, the moments of time at which the maximum values of the quantities Θ_m and $\varepsilon_m^{(0)}$ are reached, do not coincide.

The fact that in the case of nonlinear dynamic deformation of thin-walled CM-structures, deformations can reach their maximum values much later than the time of the termination of the action of an intense short-term load, is discovered for elastic shells in [6].

Comparison of curves ***1*** in Fig. 5***a*** and Fig. 5***b*** shows that the maximum values of the deformation intensity of the binder in fiberglass plates of different relative thicknesses with a 2D reinforcement structure are comparable with each other. However, a comparison of the behavior of curves ***1*** and ***1″*** curves in Fig. 3 at $M = 7$ indicates that a relatively thick structure (see curve ***1″***) heats up significantly less than a relatively thin one (see curve ***1***). This fact is explained by the fact that in a relatively thick CM-structure, the most intense deformation of the components of the composition occurs in small zones adjacent to rigidly fixed edges, and transverse shear deformations dominate in these zones. In relatively thin CM-plates, the main part of the structure (remote from the supporting edges), in which bending deformations dominate, is deformed most intensively. Therefore, in relatively thin plates, mechanical energy as a whole is more actively dissipated into thermal energy than in relatively thick structures, even at comparable levels of maximum deformations in their components of the composition.

All the results discussed above were obtained with taking into account the thermal sensitivity of the materials of the composition. Calculations performed without taking into account the thermal sensitivity (when the values of the characteristics of the materials of the composition given in the Table 1 at the temperature of the natural state $\Theta^0 = 20\,^\circ$C are used) show that the dependences $\Theta_m(t)$ and $\varepsilon_m^{(0)}(t)$, at the same time, visually almost do not differ from the curves shown in Fig. 3, Fig. 4 and Fig. 5***a*** – Fig. 5***c***. This is explained by a small increment of temperature under dynamic elastoplastic deformation of the considered CM-structures (by only 2÷30°C) due to the action of an explosive-type load. Note that a similar level of heating (about 10°C) is also observed in experiments on shock loading of samples from homogeneous materials [4, 5].

In view of the low level of heating of the considered CM-structures, it is advisable to compare the above results with the calculations performed according to the elastoplastic theory [21], i.e. with complete neglect of the thermal effect. It was established that for the investigated CM-plates, the results of such calculations for deflections (the corresponding dependences are not shown) visually do not differ from the calculations performed according to thermoelastoplastic theory. However, there is some (sometimes significant) difference for dependencies $\varepsilon_m^{(0)}(t)$. So, curve ***2*** in Fig. 5***d*** coincides with curve ***2*** in Fig. 5***c*** (this is the same curve), and curve ***2′*** in Fig. 5***d*** was obtained under the same conditions as curve ***2***, but without taking into account this effect. The ordinate of the global maximum point (at $t \approx 1.85$ ms) on curve ***2′*** is less than the same value on curve ***2*** by 8.8%. Note that the calculation performed according to the thermoelastoplastic theory taking into account the thermal sensitivity of the components of the composition, but at $M = 2$ (see (59)), leads to a dependence $\varepsilon_m^{(0)}(t)$ that almost does not differ from curve ***2′*** in Fig. 5***d***. Hence, in the case of relatively thin metal-composite plates, neglect of the thermal effect or the calculation of temperature fields with a rough

accuracy can lead to a significant (more than 5%) underestimation of the calculated values of the intensity of deformations of the composition components. In the case of fiberglass plates, the maximum values of the intensity of deformations of the components of the composition, obtained with and without taking into account the thermal effect, practically do not differ. Therefore, the dynamic elastoplastic behavior of thin-walled fiberglass structures can be reasonably calculated without taking into account the thermal effect.

In Fig. 5 was not shown the dependences $\varepsilon_{\mathrm{m}}^{(k)}(t)$ for fibers of the k-th family ($1 \le k \le N$), as if they are qualitatively similar to the curves shown in Fig. 5 for the bonding material, but have lower values along the ordinate axis. In particular, for fibers of the second family ($k = 2$), which experience the largest deformations, the maximum values $\varepsilon_{\mathrm{m}}^{(2)}$ are approximately 1.5÷1.7 times less than for the dependences shown in Fig. 5.

Conclusion. A model of thermoelastoplastic deformation of flexible plates with arbitrary structures of reinforcement has been developed, which enable one to take into account the possible weak resistance of such structures to transverse shears and the connectivity of thermophysical and mechanical problems. An explicit numerical scheme for integrating the formulated coupled initial-boundary value problem has been developed. It is established that the time step is determined from the Courant stability criterion for the wave equation, and not from the stability criterion of the numerical scheme for two-dimensional heat balance equations.

It is established that for an adequate calculation of the temperature fields in CM-plates under their dynamic elastoplastic bending deformation, the temperature in the transverse direction must be approximated by polynomials of the 6th or 7th orders.

Calculations have shown that under dynamic loading of CM-plates by a transverse explosive-type load , fiberglass structures are heated up no more than 2÷18°C, and metal-composite structures are heated up no more than 30°C. In this case, relatively thin plates are heated to a greater extent than relatively thick ones, even with comparable values of the highest values of the deformation intensities of the components of the composition.

Replacing a plane orthogonal structure of reinforcement (Fig. 1***a***) with a spatial structure of reinforcement (Fig. 1***b***), while maintaining the total consumption of fibers in a relatively thick fiberglass plate, enable one to reduce the intensity of deformation of the binder material by two times, however, the highest temperature value increases, although insignificantly (from 1.5 to 2.5°C). A similar replacement of structures of reinforcement in relatively thin fiberglass, as well as in relatively thin and relatively thick metal-composite structures is ineffective, as if it leads to an increase in the maximum values of the intensity of binder deformations and increments of temperature in CM-plates.

To carry out adequate dynamic calculations of fiberglass plates, flexurally deformed by a load due to an air blast wave, it is quite reasonable to ignore the effect of thermal action if there are no additional sources of heating or cooling of non-mechanical origin.

However, in metal-composite thin-walled structures under such loading, taking into account the thermal effect is mandatory (although the thermal sensitivity of the components of the composition can be ignored in this case), otherwise the calculations can lead to a significant underestimation of the deformed state of the components of the composition. In this case, the traditional approximation of the temperature over the thickness of the plates in the form of a square parabola also leads to inadequate calculation results, similar to the complete neglect of the thermal effect.

The work was carried out within the framework of a state assignment (state registration No. 121030900260-6).

1. *Абросимов Н. А., Баженов В. Г.* Нелинейные задачи динамики композитных конструкций. – Нижний Новгород: Изд-во ННГУ, 2002. – 400 с.
2. *Амбарцумян С. А.* Теория анизотропных пластин. Прочность, устойчивость и колебания. – Москва: Наука, 1987. – 360 с.
3. *Безухов Н. И., Бажанов В. Л., Гольденблат И. И., Николаенко Н. А., Синюков А. М.* Расчеты на прочность, устойчивость и колебания в условиях высоких температур. – Москва: Машиностроение, 1965. – 568 с.
4. *Белл Дж. Ф.* Экспериментальные основы механики деформируемых твердых тел: В 2 ч. – Часть I. Малые деформации. – Москва: Наука, 1984. – 597 с
5. *Белл Дж. Ф.* Экспериментальные основы механики деформируемых твердых тел: В 2 ч. – Часть II. Конечные деформации. – Москва: Наука, 1984. – 432 с.
6. *Богданович А. Е.* Нелинейные задачи динамики цилиндрических композитных оболочек. – Рига: Зинатне, 1987. – 295 с.
7. *Грешнов В. М.* Физико-математическая теория больших необратимых деформаций металлов. – Москва: Физматлит, 2018. – 232 с.
8. *Жигун И. Г., Душин М. И., Поляков В. А., Якушин В. А.* Композиционные материалы, армированные системой прямых взаимно ортогональных волокон. 2. Экспериментальное изучение // Механика полимеров. – 1973. – № 6. – С. 1011–1018.
9. *Киселев С. П.* Механика сплошных сред: Учеб. пособие. – Новосибирск: Изд-во НГТУ, 2017. – 164 с.
10. *Композиционные* материалы. Справочник / Под ред. Д. М. Карпиноса. – Киев: Наук. думка, 1985. – 592 с.
11. *Кудинов А. А.* Тепломассообмен: Учеб. пособие. – Москва: ИНФРА-М, 2012. – 375 с.
12. *Кудинов В. А., Кудинов И. В.* Методы решения параболических и гиперболических уравнений теплопроводности / Под ред. Э. М. Карташова. – Москва: Либроком, 2012. – 280 с.
13. *Луканин В. Н., Шатров М. Г., Камфер Г. М., Нечаев С. Г., Иванов И. Е., Матюхин Л. М., Морозов К. А.* Теплотехника: Учеб. для вузов / Под ред. В. Н. Луканина. – Москва: Высш. шк., 2003. – 672 с.
14. *Новицкий Л. А., Кожевников И. Г.* Теплофизические свойства материалов при низких температурах. Справочник. – Москва: Машиностроение, 1975. – 216 с.
15. *Рихтмайер Р., Мортон К.* Разностные методы решения краевых задач. – Москва: Мир, 1972. – 418 с.
    То же: *Richtmyer R. D., Morton K. W.* Difference methods for initial-value problems. – New York etc.: Intersci. Publ., 1967. – xiv+405 p.
16. *Справочник* по композитным материалам: В 2 кн. – Кн. 1 / Под ред. Дж. Любина. – Москва: Машиностроение, 1988. – 448 с.
    То же: *Handbook* of composites / Ed. G. Lubin. – New York: Van Nostrand Reinhold, 1982. – xi+786 p.
17. *Тарнопольский Ю. М., Жигун И. Г., Поляков В. А.* Пространственно-армированные композиционные материалы: Справочник. – Москва: Машиностроение, 1987. – 224 с.
18. *Хажинский Г. М.* Модели деформирования и разрушения металлов. – Москва: Научный мир, 2011. – 231 с.
19. *Шустер Й., Гейдер Д., Шарп К., Глования М.* Измерение и моделирование теплопроводности трехмерных тканых композитов // Механика композитн. материалов. – 2009. – **45**, № 2. – С. 241–254.
20. *Янковский А. П.* Вязкоупругопластическое деформирование пластин с пространственными структурами армирования // Прикл. механика и технич. физика. – 2020. – **61**, № 1. – С. 118–132.
21. *Янковский А. П.* Моделирование упругопластического деформирования гибких пологих оболочек с пространственными структурами армирования // Вычисл. механика сплошных сред. – 2018. – **11**, № 3. – С. 335–354.
22. *Houlston R., DesRochers C. G.* Nonlinear structural response of ship panels subjected to air blast loading // Comput. & Struct. – 1987. – **26**, No. 1-2. – P. 1–15.
23. *Reddy J. N.* Mechanics of laminated composite plates and shells: Theory and analysis. – Boca Raton: CRC Press, 2003. – 858 p.
24. *Yankovskii A. P.* Modeling of thermoelastoplastic deformation of reinforced plates. I. Structural model of the reinforced medium // Мат. методи та фіз.-мех. поля. – 2021. – **64**, № 1. – С. 137–148.

МОДЕЛЮВАННЯ ТЕРМОПРУЖНОПЛАСТИЧНОГО ДЕФОРМУВАННЯ АРМОВАНИХ ПЛАСТИН. II. ПОСТАНОВКА ЗАДАЧІ ТА МЕТОД РОЗВ'ЯЗУВАННЯ

Сформульовано зв'язану початково-крайову задачу термопружнопластичного деформування гнучких армованих пластин. Можливий слабкий опір таких конструкцій поперечному зсуву враховується в рамках теорії Амбарцумяна. Геометрична нелінійність враховується у наближенні Кармана. Температура по товщині пластин апроксимується поліномами різних порядків. Розв'язок сформульованої двовимірної задачі будується з використанням явної чисельної схеми. Досліджено динамічну термопружнопластичну поведінку плоско-перехресно і просторово армованих склопластикових і металокомпозитних пластин, згинальних під дією повітряної вибухової хвилі. Показано, що для адекватного визначення температури в таких конструкціях її необхідно апроксимувати поліномами 6–7-го порядків по товщині пластин. Продемонстровано, що відносно тонкі композитні пластини нагріваються більше, ніж відносно товсті при однакових максимальних значеннях інтенсивності деформацій в зв'язуючому. Рівень нагріву армованих конструкцій незначний: для склопластикових пластин приріст температури становить 2÷18°C, а для металокомпозитних конструкцій – 30°C. Тому динамічний розрахунок склопластикових пластин при дії навантажень типу повітряної вибухової хвилі можна проводити без урахування теплової дії при відсутності додаткових джерел тепла немеханічного походження. При розрахунках металокомпозитних пластин необхідно враховувати теплову дію, але термочутливість можна не враховувати.

Ключові слова: *гнучкі пластини, плоске армування, просторове армування, динамічний згин, теорія Амбарцумяна, термопружнопластичне деформування, навантаження вибухового типу, явна числова схема.*

Khristianovich Institute of theoretical
and applied mechanics, Siberian Branch of Russian
Academy of Sciences, Novosibirsk, Russia

Received
18.01.21